Multiple autoresonance accelerations generated from a chaotic base

Y. Gell
CET, P.O. Box 39513, Tel-Aviv 61394, Israel

R. Nakach
Département de Recherches sur la Fusion Contrôlée, Association Euratom—Commissariat à l'Energie Atomique, Centre d'Etudes de Cadarache, 13108 St. Paul lez Durance Cedex, France

(Received 20 September 1996)

A multiple autoresonance process for accelerating electrons is presented. It is based on the autoresonance mechanism put forth in a previous publication [Y. Gell and R. Nakach, Phys. Lett. A **207**, 342 (1995)]. The configuration under study consists of two circularly polarized electromagnetic waves propagating in opposite directions along a constant magnetic field and having frequencies in the electron frequency range. Such a configuration admits, under appropriate conditions, stochastic motion of the particle. It is shown that the stochastic nature of the motion plays an important role for inducing the multiple autoresonance acceleration. The threshold for the onset of stochasticity when considering waves with different characteristics and particles with different initial conditions is evaluated and compared with the numerical data. It is shown that for a proper choice of the parameters of the system, the multiple autoresonance process can generate a bulk of particles moving in a preferential direction and having a considerable time-averaged velocity parallel to the magnetic field. Practical applications of this result are mentioned. [S1063-651X(97)12305-4]

PACS number(s): 52.35.Nx, 52.20.Dq, 05.45.+b, 52.50.Gj

I. INTRODUCTION

The autoresonance (AR) interaction has recently been attracting a large amount of interest both as a possible candidate for accelerating particles [1,2] as well as for fusion current drive [3] and in electron cyclotron heating of plasmas [4]. The limitations of AR mechanism are very well known, namely, (a) the necessity of having exact appropriate initial conditions for this mechanism to be operational and (b) the necessity of having the refractive index of the medium of the propagating waves equal to one. Attempts to overcome these limitations have been reported in the literature [5–7]. For more details and references regarding these investigations the reader is referred to Ref. [6].

In a recent publication [8] we have shown that there is a possibility to remedy the first shortcoming inherently associated with this process by a mechanism that allows for particles far away from the AR conditions to get pushed into these conditions, staying there for a considerable length of time. In Ref. [8] we limited ourselves to a specific configuration of two circularly polarized electromagnetic (e.m.) waves having the same amplitudes, wave numbers, and frequencies propagating in vacuum in opposite directions, thus considering essentially a standing-wave configuration. An intrinsic feature of the relativistic dynamics of electrons in such a configuration is the appearance of chaotic motion manifested as a spread out band in the associated phase space. However, this stochastic motion does not necessarily prevail indefinitely since the particle, due to a possible AR capture, might leave the stochastic sea and undertake a regular motion. This unexpected phenomenon might have promising applications, which we will mention later on.

The significance of our results might be somewhat restrictive due to the special configuration considered in Ref. [8], namely, the simplifying conditions associated with a standing-wave configuration. In this paper, we show that the transition from chaotic to regular entrainment is fundamental to the two-e.m.-wave configuration, the standing-wave case being only a particular example. The importance of this generalization of the phenomenon lies in the flexibility it renders to explore large portions of phase space searching for stochasticity. By choosing properly the parameters of the waves, one allows for an enhanced population of particles to have a chance to participate in AR acceleration, resulting thus in an efficient way of transferring energy and momentum from the waves to the particles. Implications of this process could be of importance for the current generation and heating of plasmas in thermonuclear fusion projects.

This general transition process from chaotic motion to AR acceleration is exposed and explored in Sec. II, where we solve numerically the equations of motion for various parameters and initial conditions of the system. In order to exhibit clearly the essential features of this process, we present the solutions of equations of motion both in real time and in phase space. A convenient formalism for analyzing and presenting phase-space characteristics of the motion of the system is to use an Hamiltonian function expressed in action angle variables. In a phase-space representation of these variables, time is of course eliminated. However, much insight can be gained when time evolution of the action variables is explicitly exhibited. We thus present the time dependence of the two actions in the same graph, which allows one to recognize favorable conditions for possible applications, as we will explain later on. This type of graph also reveals regular motions when the amplitudes of the waves are below threshold for stochasticity, chaotic motion when this threshold is crossed, and a transition state between stochastic and regular motion when AR capture is about to occur.

The possible existence of a chaotic band in phase space is rather fortunate since it allows for particles being far away

from the appropriate conditions for AR capture to wander and reach these privileged conditions. As the stochastic behavior of the motion of the particle is important for fulfilling, on a large scale, the requirements necessary for the AR acceleration of the electrons, it is desirable to have a straightforward efficient way to detect the appearance of stochasticity. This is readily accomplished by utilizing the usual surface of section technique.

The prediction of the onset of this stochastic behavior in phase space is an essential part of the analysis of this problem and is dwelled upon in some detail in Sec. III. In that section we derive approximate theoretical expressions for the threshold, depending on the whole set of parameters and initial conditions. These predictions are compared then with the numerical results obtained from the solutions of the equations of motion. The limitations and shortcomings of the predictive power of these expressions are discussed in detail.

The fact that one can use an asymmetric configuration of waves and still have the AR entrainment process operative allows for an acceleration of an ensemble of particles in a preferential direction. It is found that the time-averaged parallel velocity of the particles can be very significant due to an accumulation in time of accelerating steps and can thus result in the generation of a current. A discussion of these aspects of the analysis constitutes the major part of Sec. IV of this paper, in which we also outline avenues for future research.

II. STOCHASTICALLY INDUCED AUTORESONANCE PROCESSES

The important role that stochasticity plays in moving particles to bring them in AR trapping regions in phase space is motivating our research for appropriate schemes for generating stochastic motion of the particle. As is well known [1], a single circularly polarized wave propagating parallel to a magnetic field cannot serve as a candidate for this purpose since such a system is completely integrable. However, introducing an additional e.m. wave also circularly polarized propagating in the opposite direction of the first wave can lead to the generation of stochastic motion, as was shown in Ref. [8]. In this work we deal with the very specific example of a standing-wave configuration. Hereby we relax this restrictive condition and study the more general parameter space of the system. To this end we use a Hamiltonian formalism for describing the relativistic motion of an electron moving in the presence of two circularly polarized e.m. waves having, in principle, different amplitude wave numbers and frequencies and propagating along a constant magnetic field B_0 that is fixed in the z direction.

The Hamiltonian describing the dynamics of the system is expressed in the standard manner as

$$H=\{m^2c^4+(c\mathbf{P}+e\mathbf{A})^2\}^{1/2}. \tag{1}$$

The essential physics lies in the expression of the vector potential. Considering first two counterpropagating waves, the vector potential for this case will read

$$\mathbf{A}=B_0x\mathbf{e}_y+A_1\{[\sin(k_1z-\omega_1t)\mathbf{e}_x]+[\cos(k_1z-\omega_1t)\mathbf{e}_y]\}+A_2\{[-\sin(k_2z+\omega_2t)\mathbf{e}_x]+[\cos(k_2z+\omega_2t)\mathbf{e}_y]\}. \tag{2}$$

Without loss of generality, we can choose $P_y=0$ since the Hamiltonian is independent of the y coordinate. For completeness we repeat the steps leading to equations of motion as presented in Ref. [8]. Following the formalism as developed by Chen and Schmidt [9], we transform the coordinates and momenta into action angle variables via the relations

$$x=\sqrt{\frac{2Ic}{eB_0}}\sin\theta, \quad P_x=\sqrt{\frac{2IeB_0}{c}}\cos\theta.$$

Time is eliminated with the help of the generating function

$$F=(\theta-k_2z-\omega_2t)P_\psi+(\theta+k_1z-\omega_1t)P_\phi.$$

The transformed Hamiltonian expressed in normalized variables is

$$\overline{H}(\psi,\phi,P_\psi,P_\phi)=[1+\overline{A_1^2}+\overline{A_2^2}+(\overline{k_1}P_\phi-\overline{k_2}P_\psi)^2+2(P_\phi+P_\psi)+2\sqrt{2(P_\phi+P_\psi)}(\overline{A_1}\sin\phi+\overline{A_2}\sin\psi)+2\overline{A_1}\overline{A_2}\cos(\phi-\psi)]^{1/2}-\overline{\omega_1}P_\phi-\overline{\omega_2}P_\psi, \tag{3}$$

where $\overline{\psi}=\partial F/\partial P_\psi=\theta-\overline{k_2}\overline{z}-\overline{\omega_2}\overline{t}$ and $\overline{\phi}=\partial F/\partial P_\phi=\theta+\overline{k_1}\overline{z}-\overline{\omega_1}\overline{t}$, and the normalized actions I and P_z are expressed in terms of the new momenta as

$$\overline{I}=\frac{\partial F}{\partial\theta}=P_\phi+P_\psi, \quad \overline{P_z}=\frac{\partial F}{\partial\overline{z}}=\overline{k_1}P_\phi-\overline{k_2}P_\psi. \tag{4}$$

The normalizations of the other quantities are $\overline{H}=H/mc^2$, $\overline{A_{1,2}}=eA_{1,2}/mc^2$, $\overline{P_z}=P_z/mc$, $\overline{t}=\Omega t$, $\overline{\omega_{1,2}}=\omega_{1,2}/\Omega$, $\overline{k_{1,2}}=k_{1,2}c/\Omega$, $\overline{z}=\Omega z/c$, $\overline{I}=I\Omega/mc^2$, and $\overline{P_\perp}=P_\perp/mc=\sqrt{2\overline{I}}$, Ω being the gyrofrequency eB_0/mc. The Hamilton equations of motion read

$$\dot{\psi}=\frac{\partial\overline{H}}{\partial P_\psi}=\frac{1}{\gamma}\left[-\overline{k_2}(\overline{k_1}P_\phi-\overline{k_2}P_\psi)+1+\frac{\overline{A_1}\sin\phi+\overline{A_2}\sin\psi}{\sqrt{2(P_\phi+P_\psi)}}\right]-\overline{\omega_2}, \tag{5}$$

$$\dot{\phi}=\frac{\partial\overline{H}}{\partial P_\phi}=\frac{1}{\gamma}\left[+\overline{k_1}(\overline{k_1}P_\phi-\overline{k_2}P_\psi)+1+\frac{\overline{A_1}\sin\phi+\overline{A_2}\sin\psi}{\sqrt{2(P_\phi+P_\psi)}}\right]-\overline{\omega_1}, \tag{6}$$

$$\dot{P}_\psi=-\frac{\partial\overline{H}}{\partial\psi}=-\frac{\overline{A_2}}{\gamma}[\sqrt{2(P_\phi+P_\psi)}\cos\psi+\overline{A_1}\sin(\phi-\psi)], \tag{7}$$

$$\dot{P}_\phi=-\frac{\partial\overline{H}}{\partial\phi}=-\frac{\overline{A_1}}{\gamma}[\sqrt{2(P_\phi+P_\psi)}\cos\phi-\overline{A_2}\sin(\phi-\psi)], \tag{8}$$

where

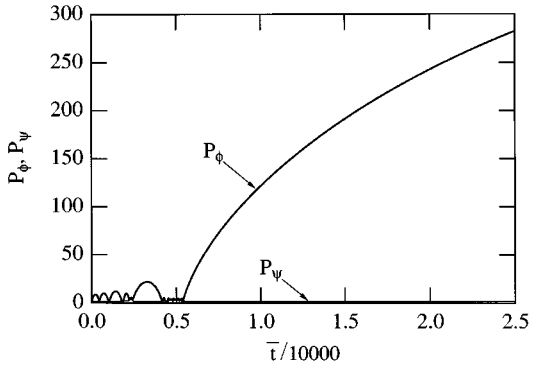

FIG. 1. Canonical actions P_ϕ and P_ψ as functions of the normalized time $\bar{t}$, for a system consisting of two circularly polarized e.m. waves propagating in opposite directions with normalized parameters $\bar{A}_1=0.07$, $\bar{A}_2=0.02$, $\bar{k}_1=0.4$, $\bar{k}_2=0.2$, $\bar{\omega}_1=0.4$, and $\bar{\omega}_2=0.2$. The initial values of the canonical action angle variables are $P_{\phi 0}=1.6$, $P_{\psi 0}=1.5$, $\phi_0=3.1$, and $\psi_0=3.1$. Symbols and normalization are as defined in the text. The heavy and thin lines correspond to the actions P_ϕ and P_ψ, respectively.

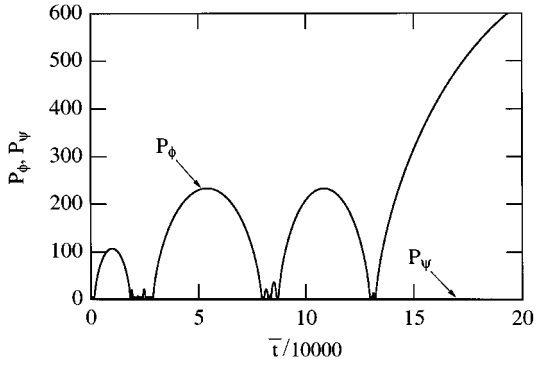

FIG. 2. Same as Fig. 1. The only change is in the initial conditions for the actions, which now read $P_{\phi 0}=3.7$ and $P_{\psi 0}=4.5$.

$$\gamma=[1+(\bar{k}_1P_\phi-\bar{k}_2P_\psi)^2+2(P_\phi+P_\psi)+\bar{A}_1^2+\bar{A}_2^2 +2\sqrt{2(P_\phi+P_\psi)}(\bar{A}_1\sin\phi+\bar{A}_2\sin\psi) +2\bar{A}_1\bar{A}_2\cos(\phi-\psi)]^{1/2} =\bar{H}+\bar{\omega}_1P_\phi+\bar{\omega}_2P_\psi. \tag{9}$$

Note that the Hamiltonian $\bar{H}$ is independent of time; it is thus a constant of motion and is determined by the parameters and initial values of the system. This system not being integrable forces us to analyze its solutions by using numerical techniques. Concentrating on the possibility to detect typical AR accelerations, we find it convenient to present the numerical solutions of the equations of motion as evolving in time. An example for such a solution is shown in Fig. 1. In this figure we consider a set of parameters that corresponds to a non-standing-wave configuration ($\bar{A}_1=0.07$, $\bar{A}_2=0.02$, $\bar{k}_1=\bar{\omega}_1=0.4$, $\bar{k}_2=\bar{\omega}_2=0.2$ assuming luminous waves, $\bar{k}_1=\bar{\omega}_1$, and $\bar{k}_2=\bar{\omega}_2$). By comparing this figure with Fig. 1 of Ref. [8], one realizes in a striking manner the nonpreferential nature of the standing-wave configuration for the operationality of the AR mechanism. Furthermore, inspecting Fig. 1, one observes a main feature of the time dependence of the two actions P_ϕ and P_ψ. Indeed, following the heavy curve corresponding to the time evolution of the action P_ϕ with the associated action P_ψ represented by the thin curve, one immediately observes that when P_ϕ starts to increase considerably the other action remains essentially constant. This correlated behavior of the two actions can be understood by inspecting the equations of motion when expressed via their original variables. Indeed, considering, for example, Eq. (6), we thus obtain

$$\frac{d\phi}{dt}=-\omega_1(1-\beta_z)+\frac{\Omega}{\gamma}[1+\bar{A}_1(\ )+\bar{A}_2(\ )],$$

where

$$\beta_z=\frac{v_z}{c}=\frac{\bar{P}_z}{\gamma}=\frac{\bar{k}_1P_\phi-\bar{k}_2P_\psi}{\gamma}. \tag{10}$$

For an exact AR condition for the wave designed by index 1, the particle obeys the well-known relation [1]

$$\gamma(1-\beta_z)=\frac{\Omega}{\omega_1}=\frac{1}{\bar{\omega}_1}. \tag{11}$$

Using then Eq. (9), we get

$$\bar{H}+\bar{\omega}_1P_\phi+\bar{\omega}_2P_\psi-(\bar{k}_1P_\phi-\bar{k}_2P_\psi)=\frac{1}{\bar{\omega}_1},$$

which results in

$$P_\psi=\frac{\frac{1}{\bar{\omega}_1}-\bar{H}}{2\bar{\omega}_2}=\text{const}\equiv P_\psi^*. \tag{12}$$

We could of course have shown an analogous result by interchanging the roles of P_ϕ and P_ψ for the AR condition $\gamma(1+\beta_z)=\Omega/\omega_2=1/\bar{\omega}_2$ and getting then the condition for AR capture as

$$P_\phi=\frac{\frac{1}{\bar{\omega}_2}-\bar{H}}{2\bar{\omega}_1}=\text{const}\equiv P_\phi^*. \tag{13}$$

Now, considering Eq. (8), since for exact AR condition the phase ϕ and the action P_ψ are constants, the integration of this equation leads to an unlimited growth of the action P_ϕ. However, exact AR is an abstraction even for a single-wave configuration due to the spread of the initial conditions; it is certainly so for a two-wave configuration. In general, one should not expect an indefinite growth of one of the actions, but rather a bell-shaped structure reflecting the slow variation in time of the corresponding phase.

Indeed, in Fig. 2 we show a typical behavior, in which we observe successive AR captures manifested as bell structures for one of the actions (the heavy curve) correlated with the essentially constancy of the associated action (the thin line). These structures are separated by time intervals where the AR is not operative and the system undergoes stochastic motion. One should realize that the two actions are on the same

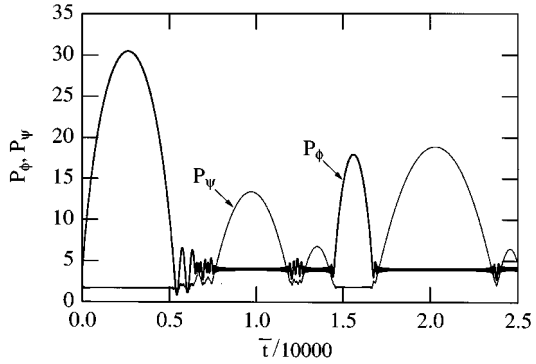

FIG. 3. Same as Fig. 1. The changes are in the following parameters and initial conditions, which now read $A_1=0.03$, $A_2=0.01$, $k_1=\omega_1=0.4$, $k_2=\omega_2=0.2$, $P_{\phi 0}=3.8$, $P_{\psi 0}=1.4$, $\phi_0=3.1$, and $\psi_0=3.1$.

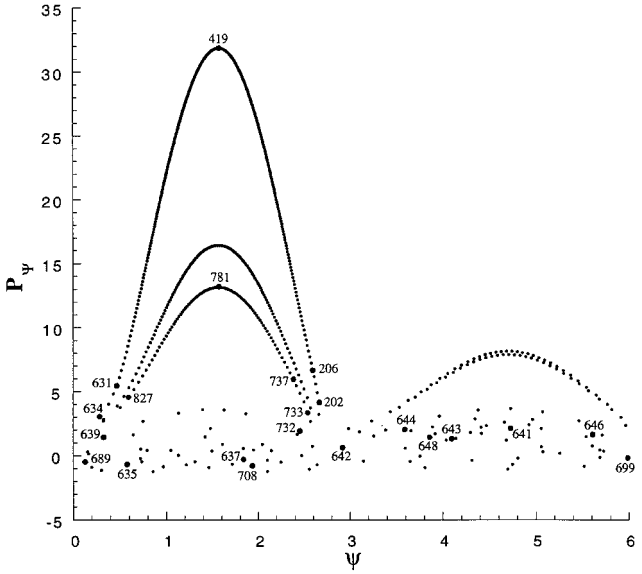

FIG. 4. Particle trajectories in phase space (P_ψ,ψ) with $\psi(\mathrm{mod}2\pi)$ viewed at successive crossings of the cut plane defined by the condition $\phi=0$. The configuration parameters and initial conditions are $A_1=0.07$, $A_2=0.05$, $k_1=0.45$, $k_2=0.4$, $\omega_1=0.45$, $\omega_2=0.4$, $P_{\phi 0}=1.6$, $P_{\psi 0}=3.1$, $\phi_0=2.1$, and $\psi_0=2.12$. Numbers associated with the given crossings correspond to the time sequence as found from the numerical calculation. The numbered crossing points have been enlarged somewhat for visualization convenience.

footing and might interchange their roles during the course of the interaction. As can be seen in Fig. 3, in an earlier stage one observes that P_ϕ changes considerably, while P_ψ stays almost constant; in a later stage, their roles are interchanged. Consequently, the parallel velocity of the particle will change its direction during the course of the motion.

The appearance of intervals of stochastic motion we have been referring to can be seen in a transparent manner when viewing the motion in phase space. To this end we solved numerically the equations of motion (5)–(8) and present the results in phase space using the surface of section technique. The cut plane we use is determined by the condition $(\phi=0,\mathrm{mod}2\pi)$. The conjugate action and angle (P_ψ,ψ) are presented as a point in this plane. Recalling that H is a constant, the points in the cut plane determine completely the dynamics of the system. In Fig. 4 we present such a phase-space portrait of the motion of the particle. Following the successive crossing points in time, we observe that the particle starts to undergo AR acceleration once it arrives at appropriate conditions of phase and action. Once it has been set into this capture course (crossing number 202) the particle completes a bell structure in phase space returning to the stochastic sea (point 635). Wandering stochastically, the particle arrives at the right conditions (point 732). It is set again into an acceleration course and so on. The wandering period in phase space (points between 635 and 732) are the intervals referred to previously as stochastic.

The mobility of the electrons provided by the existence of a stochastic region in phase space allowing for successive AR captures is a rather general property of the system under consideration. Indeed, the type of behavior seen in Fig. 4, where $A_1>A_2$ and $k_1>k_2$, holds as well as when $A_2>A_1$, as can be seen in Fig. 5, and also holds when $k_2>k_1$. However, when the condition of counterpropagation of the waves is violated and one considers copropagating waves no stochastic region is available for the particles and thus the successive bell structures, randomly generated, can no longer be realized. To see this we consider the set of equations (3)–(9) in which k_2 is replaced by $-k_2$ accounting for the copropagation of the two waves. This set will read

$$\dot{\psi}=\frac{\partial\overline{H^*}}{\partial P_\psi}=\frac{1}{\gamma}\left[\overline{k_2}(\overline{k_1}P_\phi+\overline{k_2}P_\psi)+1+\frac{\overline{A_1}\sin\phi+\overline{A_2}\sin\psi}{\sqrt{2(P_\phi+P_\psi)}}\right]-\overline{\omega_2}, \tag{14}$$

$$\dot{\phi}=\frac{\partial\overline{H^*}}{\partial P_\phi}=\frac{1}{\gamma}\left[\overline{k_1}(\overline{k_1}P_\phi+\overline{k_2}P_\psi)+1+\frac{\overline{A_1}\sin\phi+\overline{A_2}\sin\psi}{\sqrt{2(P_\phi+P_\psi)}}\right]-\overline{\omega_1}, \tag{15}$$

$$\dot{P}_\psi=-\frac{\partial\overline{H^*}}{\partial\psi}=-\frac{\overline{A_2}}{\gamma}\left[\sqrt{2(P_\psi+P_\phi)}\cos\psi+\overline{A_1}\sin(\phi-\psi)\right], \tag{16}$$

$$\dot{P}_\phi=-\frac{\partial\overline{H^*}}{\partial\phi}=-\frac{\overline{A_1}}{\gamma}\left[\sqrt{2(P_\psi+P_\phi)}\cos\phi-\overline{A_2}\sin(\phi-\psi)\right], \tag{17}$$

where

$$\begin{aligned}\gamma=&\left[1+(\overline{k_1}P_\phi+\overline{k_2}P_\psi)^2+2(P_\phi+P_\psi)+\overline{A_1^2}+\overline{A_2^2}\right.\\&+2\sqrt{2(P_\phi+P_\psi)}(\overline{A_1}\sin\phi+\overline{A_2}\sin\psi)\\&\left.+2\overline{A_1}\overline{A_2}\cos(\phi-\psi)\right]^{1/2}\\=&\overline{H^*}+\overline{\omega_1}P_\phi+\overline{\omega_2}P_\psi,\end{aligned} \tag{18}$$

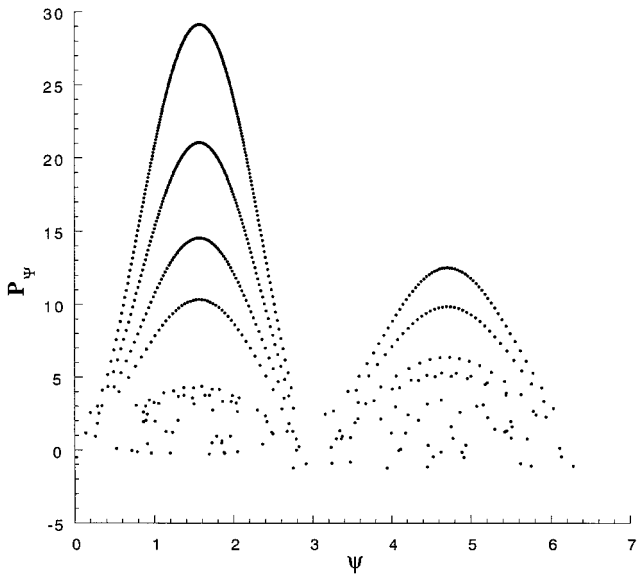

FIG. 5. Same as Fig. 4. The only change is in the amplitudes of the waves, which now read $A_1=0.048$ and $A_2=0.07$.

$\overline{H^*}$ being a constant of motion, designated specially for the copropagating case.

Considering the new time variable s defined by the relation $ds=d\overline{t}/\gamma$ and using the expression of γ as given by Eq. (18), the system of equations of motion will read

$$\psi'=\frac{d\psi}{ds}=\dot{\psi}\gamma=1-\overline{\omega_2}\overline{H^*}+(\overline{k_2^2}-\overline{\omega_2^2})P_\psi+(\overline{k_1k_2}-\overline{\omega_1}\overline{\omega_2})P_\phi+\frac{\overline{A_1}\sin\phi+\overline{A_2}\sin\psi}{\sqrt{2(P_\phi+P_\psi)}}, \tag{19}$$

$$\phi'=\frac{d\phi}{ds}=\dot{\phi}\gamma=1-\overline{\omega_1}\overline{H^*}+(\overline{k_1^2}-\overline{\omega_1^2})P_\phi+(\overline{k_1k_2}-\overline{\omega_1}\overline{\omega_2})P_\psi+\frac{\overline{A_1}\sin\phi+\overline{A_2}\sin\psi}{\sqrt{2(P_\phi+P_\psi)}}, \tag{20}$$

$$P'_\psi=\frac{dP_\psi}{ds}=\dot{P}_\psi\gamma=-\overline{A_2}\sqrt{2(P_\phi+P_\psi)}\cos\psi-\overline{A_1}\overline{A_2}\sin(\phi-\psi), \tag{21}$$

$$P'_\phi=\frac{dP_\phi}{ds}=\dot{P}_\phi\gamma=-\overline{A_1}\sqrt{2(P_\phi+P_\psi)}\cos\phi+\overline{A_1}\overline{A_2}\sin(\phi-\psi). \tag{22}$$

Assuming $\overline{k_1}=\overline{\omega_1}$ and $\overline{k_2}=\overline{\omega_2}$ and subtracting Eq. (20) from Eq. (19), we get

$$\psi'-\phi'=(\overline{\omega_1}-\overline{\omega_2})\overline{H^*}\equiv c_0=\text{const.}$$

This constant allows us to express one phase in terms of the other as

$$\psi=\phi+c_0s+\xi_0, \tag{23}$$

where ξ_0 is a phase constant of integration. This relation allows for a decoupling of the two degrees of freedom leading to a separate interaction of the two waves with the particle, which turns out to be completely integrable. For a detailed derivation of this statement we refer the reader to the Appendix. Note that this result is still valid when the polarization of the waves is changed.

The counterpropagation of the waves is thus essential for generating stochastic motion; however, the conditions for onset of such a motion involve the whole set of parameters of the system and will be dealt in Sec. III. The location of the stochastic band in phase space considering the nonsymmetric counterpropagating waves configuration can be displaced by an appropriate change of the parameters of the system. We show this in the two frames in Fig. 6. Figure 6(a) corresponds to the parameter set $A_1=0.07$, $A_2=0.05$, $k_1=\overline{\omega_1}=0.47$, $k_2=\overline{\omega_2}=0.4$, $P_{\phi0}=1.5$, $P_{\psi0}=3.1$, $\phi_0=2.1$, and $\psi_0=2.12$, which results in a stochastic band centered around $P_\phi=0.81$. By changing the parameter set to $A_1=0.07$, $A_2=0.05$, $k_1=\overline{\omega_1}=0.35$, $k_2=\overline{\omega_2}=0.4$, $P_{\phi0}=1.6$, $P_{\psi0}=3.1$, $\phi_0=4.1$, and $\psi_0=3.12$, the center of the stochastic band is moved to $P_\phi\cong2.2$, as can be seen in Fig. 6(b). As is well known, the size of the stochastic layers depends on the magnitudes of the two waves considered. The importance of the flexibility of locating the stochastic layers in phase space will be elaborated upon in Sec. IV.

III. THRESHOLD FOR THE ONSET OF STOCHASTICITY

The system under consideration is rather rich in independent parameters as well as initial conditions fixing the motion of the particle. As such its behavior is expected to be an involved and intricated one. We then are going to search for global estimates for the conditions of the onset of stochasticity; refined estimates will be out of order here. The standard mechanism leading to a rough reliable estimate for the threshold of stochasticity is based on the notion of resonance overlap [10]. This sets the framework of our analysis. Starting from equations of motion (5)–(8), we want to transform them into a form from which the overlapping criterion can be deduced. To this end, we find it convenient here to introduce also the proper time, namely, s, defined by the relation $ds=d\overline{t}/\gamma$. The equations of motion are derived in a similar way to what was done in Sec. II and read

$$\psi'\equiv\frac{d\psi}{ds}=\dot{\psi}\gamma=1-\overline{k_2}\overline{H}-2\overline{k_1k_2}P_\phi+\frac{\overline{A_1}\sin\phi+\overline{A_2}\sin\psi}{\sqrt{2(P_\phi+P_\psi)}}, \tag{24}$$

$$\phi'\equiv\frac{d\phi}{ds}=\dot{\phi}\gamma=1-\overline{k_1}\overline{H}-2\overline{k_1k_2}P_\psi+\frac{\overline{A_1}\sin\phi+\overline{A_2}\sin\psi}{\sqrt{2(P_\phi+P_\psi)}}, \tag{25}$$

$$P'_\psi\equiv\frac{dP_\psi}{ds}=\dot{P}_\psi\gamma=-\overline{A_2}\sqrt{2(P_\phi+P_\psi)}\cos\psi-\overline{A_1}\overline{A_2}\sin(\phi-\psi), \tag{26}$$

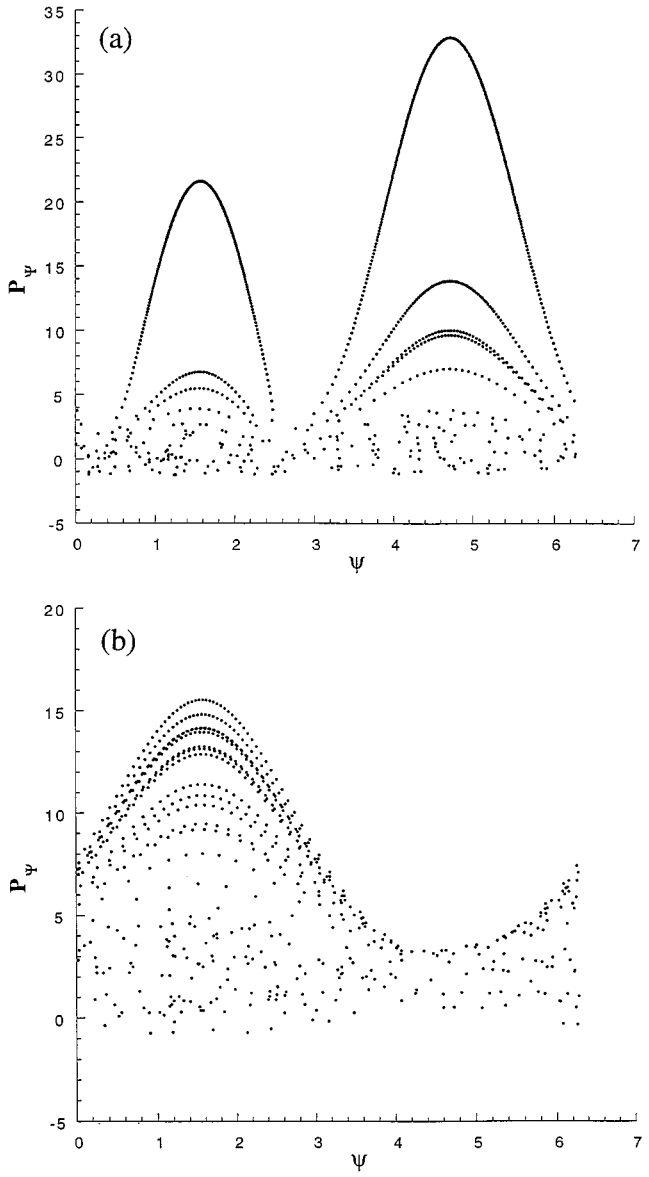

FIG. 6. Same as Fig. 4 showing the displacement of the stochastic band in phase space. (a) corresponds to the parameters $\overline{A_1}=0.07$, $\overline{A_2}=0.05$, $k_1=\overline{\omega_1}=0.47$, and $k_2=\overline{\omega_2}=0.4$, with the initial conditions $P_{\phi 0}=1.5$, $P_{\psi 0}=3.1$, $\phi_0=2.1$, and $\psi_0=2.12$. (b) corresponds to the parameters $\overline{A_1}=0.07$, $\overline{A_2}=0.05$, $k_1=\overline{\omega_1}=0.35$, and $k_2=\overline{\omega_2}=0.4$, with the initial conditions $P_{\phi 0}=1.6$, $P_{\psi 0}=3.1$, $\phi_0=4.1$, and $\psi_0=3.12$.

$$P'_\phi \equiv \frac{dP_\phi}{ds}=\dot{P}_\phi\gamma=-\overline{A_1}\sqrt{2(P_\phi+P_\psi)}\cos\phi + \overline{A_1A_2}\sin(\phi-\psi). \tag{27}$$

For future reference, we introduce the variable ξ as the difference of the phases ϕ and ψ. From Eqs. (24)–(27) one gets immediately

$$\xi'=\phi'-\psi'=2\overline{k_1k_2}(P_\phi-P_\psi)+(\overline{k_2}-\overline{k_1})\overline{H}, \tag{28}$$

$$\overline{I'}=-\sqrt{2I(A_1}\cos\phi+\overline{A_2}\cos\psi). \tag{29}$$

As can be seen by inspection, the equations of motion (24)–(27) are derivable from the Hamiltonian

$$\hat{H}=-2\overline{k_1k_2}P_\phi P_\psi+(1-\overline{k_1}\overline{H})P_\phi+(1-\overline{k_2}\overline{H})P_\psi + \sqrt{2(P_\phi+P_\psi)}[\overline{A_1}\sin\phi+\overline{A_2}\sin\psi] + \overline{A_1}\overline{A_2}\cos(\phi-\psi), \tag{30}$$

where (P_ϕ,ϕ) and (P_ψ,ψ) are conjugated pairs of action angle variables. Note that once the parameters and initial values of the system are given, the Hamiltonian describing the motion in real time H determines the Hamiltonian in proper time $\hat{H}$ through the relation

$$\hat{H}=\frac{\overline{H^2}-1-\overline{A_1^2}-\overline{A_2^2}}{2}.$$

Considering the phase space associated with the conjugated pair (P_ϕ,ϕ), we want to know under what conditions the phase ϕ will undertake a stochastic behavior. To this end we derive the fundamental equation governing the change of this phase. Thus, taking the derivative with respect to the proper time s of Eq. (25) and using the whole set of equations of motion, one obtains straightforwardly the equation

$$\phi''=\overline{A_1}\frac{(1-\overline{k_1H}-2\overline{k_1k_2}P_\psi)}{\sqrt{2(P_\phi+P_\psi)}}\cos\phi + \overline{A_2}\frac{[1-\overline{k_2H}+2\overline{k_1k_2}(2P_\psi+P_\phi)]}{\sqrt{2(P_\phi+P_\psi)}}\cos\psi + 2\overline{k_1k_2A_1A_2}\sin(\phi-\psi) + \frac{(\overline{A_1}\sin\phi+\overline{A_2}\sin\psi)(\overline{A_1}\cos\phi+\overline{A_2}\cos\psi)}{P_\phi+P_\psi}. \tag{31}$$

Considering $\overline{A_1}$ and $\overline{A_2}$ to be small quantities, we group the terms on the right-hand side of this equation in first order and second order in these quantities. Equation (31) will read

$$\phi''=l_0\cos\phi+l_1\cos\psi+[O(2)\ \text{terms}], \tag{32}$$

where

$$l_0\equiv\overline{A_1}\frac{1-\overline{k_1H}-2\overline{k_1k_2}P_\psi}{\sqrt{2(P_\phi+P_\psi)}},$$

$$l_1\equiv\overline{A_2}\frac{1-\overline{k_2H}+2\overline{k_1k_2}(2P_\psi+P_\phi)}{\sqrt{2(P_\phi+P_\psi)}}.$$

Second-order quantities, when not resonating can be neglected. Under such conditions, we can write approximately the equation governing the change in the phase ϕ,

$$\phi''=l_0\cos\phi+l_1\cos(\phi-c_1s+\xi_1), \tag{33}$$

where $c_1=2\overline{k_1k_2}(P_\phi-P_\psi)+(\overline{k_2}-\overline{k_1})\overline{H}$ and ξ_1 is a phase constant of integration. In deriving this equation use has been made of Eq. (28), assuming P_ϕ and P_ψ to be constant terms and taken to have their initial values $P_{\phi 0}$ and $P_{\psi 0}$.

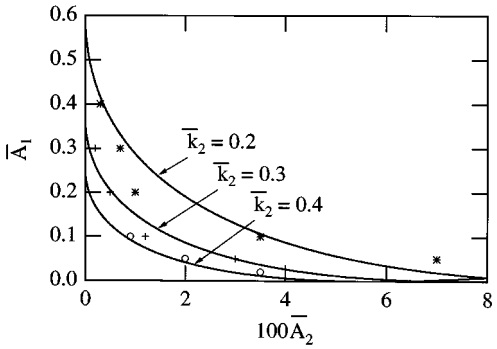

FIG. 7. Normalized threshold values of $\bar{A_1}$ and $\bar{A_2}$ for which stochasticity sets in according to Eq. (34) for a particle having the initial conditions $P_{\phi 0}=0.3$, $P_{\psi 0}=1.25$, $\phi_0=3.5$, $\psi_0=3.1$, and $\bar{k_1}=0.6$. The different curves correspond to three different values of $\bar{k_2}$ (0.2, 0.3, and 0.4), indicated in the figure. The points represented by the symbols $*$, $+$, and $\bigcirc$ correspond to the threshold values found from the numerical data; $\bar{k_2}=0.2$, 0.3, and 0.4, respectively.

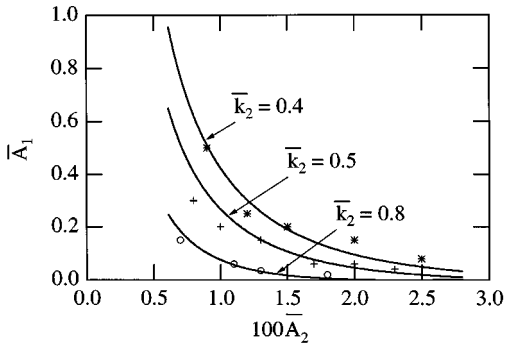

FIG. 8. Normalized threshold values of $\bar{A_1}$ and $\bar{A_2}$ for which stochasticity sets in according to Eq. (38) for a particle having the initial conditions $P_{\phi 0}=0.08$, $P_{\psi 0}=0.06$, $\phi_0=3.5$, $\psi_0=3.1$, and $\bar{k_1}=0.6$. The different curves correspond to three different values of $\bar{k_2}$ (0.4, 0.5, and 0.8). The points represented by the symbols $*$, $+$, and $\bigcirc$ correspond to the threshold values found from the numerical data, $\bar{k_2}=0.4$, 0.5, and 0.8, respectively.

Such an assumption is consistent with keeping only first-order quantities since their deviations from initial conditions are by themselves first-order quantities. Under this same assumption, l_0 and l_1 are constant quantities. Equations of the form (33) have been treated extensively in the literature, now being textbook material. We quote thus here the theoretical expression for the threshold for stochasticity for such a case [11].

$$\sigma_1=\frac{2\sqrt{l_0}+2\sqrt{l_1}}{c_1}\geqslant 0.67. \tag{34}$$

In order to test the validity of our analysis, we solve numerically the equations of motion searching for the threshold values of the amplitudes of the waves for which stochasticity sets in. In Fig. 7 we plot, for a given set of initial conditions, the threshold values of A_2 and A_1, which induce stochastic motion, considering some representative values of the wave numbers k_1 and k_2. The full curves in this figure give the threshold values as predicted by Eq. (34), the numerical data are given by the graphical symbols (see caption) corresponding, respectively, to the cases $k_2=0.2$, 0.3, and 0.4. As is seen from this figure, the agreement is quite reasonable. However, by changing significantly the initial values, especially those of the actions, the agreement deteriorates considerably. In order to understand this discrepancy we have to go back to the assumptions underlying our derivation of the threshold given in Eq. (34). By inspecting both the initial conditions and structure of the terms in Eq. (31), one realizes immediately that choosing $P_{\phi 0}$ and $P_{\psi 0}$ very small, we have underminded the ordering scheme we have proposed. Indeed, if $P_{\phi 0}+P_{\psi 0}$ is too small, the last terms that have been considered of second order attain now values comparable to the values of l_0 and l_1. Moreover, by choosing $P_{\phi 0}+P_{\psi 0}$ small we let the two initial frequencies be of comparable magnitude and their difference rather small. This permits for the beat frequency ξ' to be slowly varying, which is a characteristic of a resonating behavior. This resonating term $2k_1k_2A_1A_2\sin(\phi-\psi)$ might be even the leading term in Eq. (31), thus breaking our proposed ordering scheme. For such a case the natural variable to consider will be ξ, and one has to proceed to derive its governing equation in order to arrive at the appropriate threshold for stochasticity. To this end we derive with respect to s Eq. (28), and using Eqs. (26) and (27) one finds immediately

$$\xi''=4\overline{k_1k_2A_1A_2}\sin\xi-2\overline{k_1k_2}\sqrt{2(P_\phi+P_\psi)}\times[(\overline{A_1}\cos\phi-\overline{A_2}\cos\psi)]. \tag{35}$$

Inspecting Eqs. (24) and (25) for ψ' and ϕ', one observes that for small values of the initial actions $P_{\phi 0}$ and $P_{\psi 0}$ for which the previous criterion has failed, one gets rather high values for these frequencies, although their difference is rather small. On the time scale of variation of ξ, ϕ, and ψ thus oscillate fastly and their averaged behavior is to be looked at. Applying such a procedure to Eq. (29) yields immediately the approximate constancy of the sum of the actions I. Now we rewrite Eq. (35), expressing the dynamical phases ϕ and ψ, exhibiting explicitly their deviation from the central phase ξ as

$$\xi''=4\overline{k_1k_2A_1A_2}\sin\xi-2\overline{k_1k_2}\sqrt{2(P_\phi+P_\psi)}\times[\overline{A_1}\cos(\xi+\psi)-\overline{A_2}\cos(\xi-\phi)]. \tag{36}$$

This governing equation describes the variation of ξ due to three oscillating terms. Resonance motion can, in principle, be associated with every one of these oscillations and can be represented as islands in phase space. We thus expect three island structures: one centered around zero frequency and the other two shifted with respect to this central island on both its sides. However, their distance from this central island will be different, reflecting the difference in frequency ϕ' and ψ'. From our previous experience [12], we know that onset of stochasticity is determined by the overlap of the central island with its most neighboring one; the more distant island plays a secondary role and can be neglected. For practical purposes, considering, for example, the parameters of Fig. 8, we thus end up with the equation

$$\xi''=4\overline{k_1k_2A_1A_2}\sin\xi+2\overline{k_1k_2A_2}\sqrt{2(P_\phi+P_\psi)}\times\cos(\xi-\omega_{\phi 0}s-\varphi_0), \tag{37}$$

where $\omega_{\phi 0}=-2\overline{k_1k_2}P_{\psi 0}+1-\overline{k_1H}$, φ_0 is a constant of integration phase, and fast oscillating terms have been neglected in Eq. (36). Equation (37) is similar to Eq. (33) and leads to the threshold condition

$$\sigma_2=\frac{2\sqrt{4\overline{k_1k_2A_1A_2}}+2\sqrt{2\overline{k_1k_2A_2}\sqrt{2(P_{\phi 0}+P_{\psi 0})}}}{\omega_{\phi 0}}\geqslant 0.67. \tag{38}$$

We test this criterion for the onset of stochasticity by comparing it with the numerical data. This comparison is shown in Fig. 8. As can be seen from this figure, the agreement is quite satisfactory. The validity of this criterion is of course not limited to the specific set of parameters considered in Fig. 8, but holds generally when the underlying conditions and limitations as stated above are met. Note, finally, that since the phases ϕ and ψ play symmetric roles, they could have been interchanged, leading to an expression for the threshold equivalent to the one given in relation (34) when fulfilling the appropriate conditions.

IV. APPLICATIONS OF AUTORESONANCE ACCELERATION

The possibility of creating a stochastic band removes one of the major obstacles of applying the AR process for useful purposes. This stems from the fact that due to the existence of a stochastic region in phase space, the electrons acquire a mobility that enables them to arrive at favorable conditions for AR interaction they did not possess originally. These observations are based on the analysis of the system considering the waves propagating in vacuum ($n=1$). For a propagating medium characterized by an index different from 1, but still very close to 1, our conclusions are still valid. However, the pronounced bell structure of the action becomes reduced somewhat as compared to the $n=1$ case.

This feature is shown in Fig. 9, where we present a phase-space plot (P_ψ,ψ) for the case: $n=1.1$. As is clearly seen in this figure, two rather broad bell structures spread out on a large part of the $[0,2\pi]$ phase range are generated from the stochastic layer. When considering plasmas with higher and higher index of refraction, the effectiveness of the AR mechanism reduces until it ceases to be operative when reaching high values of n. Accordingly, the bells in the phase space reduce until they essentially disappear. A detailed analysis regarding the validity and limitation of the multiple autoresonance entrainment mechanism for the case $n\neq 1.1$ is planned to be presented in a future paper. Here we consider plasmas for which the AR mechanism is operative and note that the simultaneous appearance of a pronounced bell structure for one of the actions, while the other one remains essentially constant, has important implications regarding the velocity limit the particle can attain. Indeed, considering the expression for β_z as given in Eq. (10) and writing conveniently β_z as

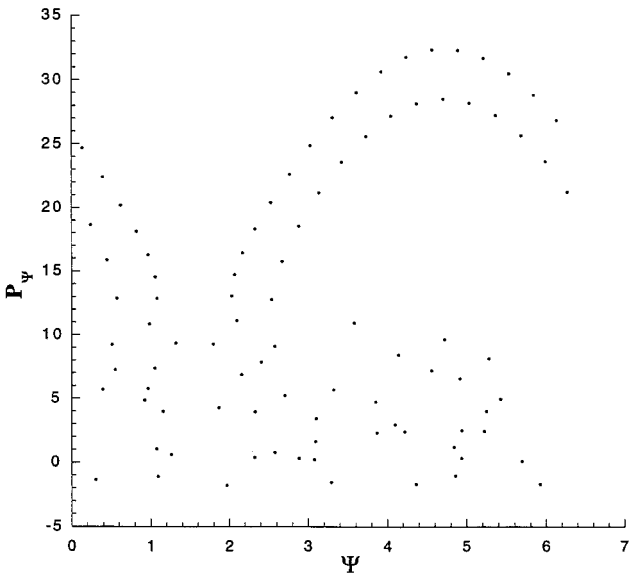

FIG. 9. Particle trajectories in phase space (P_ψ,ψ) with ψ (mod2π) as in Fig. 4, with the indices of refraction different from 1. The configuration parameters and initial conditions are $n=1.1$, $A_1=0.07$, $A_2=0.21$, $\overline{k_1}=0.33$, $\overline{k_2}=0.33$, $\overline{\omega_1}=0.3$, $\overline{\omega_2}=0.3$, $P_{\phi 0}=1.2$, $P_{\psi 0}=3.1$, $\phi_0=2.0$, and $\psi_0=4.61$.

$$\beta_z=\frac{v_z}{c}=\frac{\overline{P_z}}{\gamma}=\frac{\overline{k_1}P_\phi-\overline{k_2}P_\psi}{\overline{H}+\overline{k_1}P_\phi+\overline{k_2}P_\psi},$$

one notices that when P_ϕ, say, increases greatly while P_ψ is about constant, β_z tends to 1.

The time-averaged parallel velocity of the particle during the AR process is considerably higher than the upper border of the stochastic band from which it was emitted. The validity of this observation is based on the asymmetry in the bell direction with respect to the stochastic layer of one of the actions. Explicitly, we show that when one action, say, P_ϕ, undergoes an AR process it cannot attain values below a fixed minimum bound, while in the positive direction it can have, in principle, an unlimited grow. Indeed, when P_ϕ undergoes an AR interaction, relation (11) is approximately valid, thus $\gamma(1-\beta_z)=\gamma-k_1P_\phi+k_2P_\psi\cong 1/k_1$. Eliminating P_ψ by using relation (4) we get $k_1P_\phi\cong k_2(I-P_\phi)+\gamma-1/k_1$ and $P_\phi\cong(k_2I+\gamma-1/k_1)/(k_1+k_2)$. Since I takes only positive values and $\gamma\geqslant 1$, P_ϕ cannot reach AR values below $P_{\phi,\min}=(1-1/k_1)/(k_1+k_2)$. Similarly, when P_ψ undergoes an AR interaction, its minimum attainable value will be $P_{\psi,\min}=(1-1/k_2)/(k_1+k_2)$.

The asymmetry ascertained by the last argument still does not guarantee a preferential direction of motion for the particle, since, as we have shown in Fig. 3, the particle can in the course of its motion change its parallel directionality. However, for a large bulk of particles one can avoid this possibility by choosing properly the parameters of the waves. The criterion for such a proper choice is to have conditions appropriate for having multiple AR captures fulfilled for one action but not for the other. We recall that these conditions are that (a) the motion should be stochastic and (b) the values of the actions in the stochastic range should be such that the appropriate AR condition given by Eq. (12) or (13) is ap-

proximately fulfilled. We thus have to choose these parameters so that the width of the stochastic band will be such that this layer will be outside the range for AR capture for one of the actions and not for the other. For example, to avoid structures such as those in Fig. 3, we should choose parameters such that the upper bound of the stochastic layer, for the momentum P_ϕ, lies in the range 1.75–4.00.

Choosing properly the parameters of the waves, we thus can generate a bulk of particles moving in a preferential direction, having a considerable time-averaged parallel velocity. The possibility to have such a unidirectional motion is of course the key to generating a current drive in a plasma. Moreover, let us note that during an AR process, no substantial amount of energy or momentum is transferred from the waves to the particle in the perpendicular direction. Indeed, considering the explicit expression for $v_\perp$,

$$\frac{v_\perp}{c}=\frac{\overline{P_\perp}}{\gamma}=\frac{\sqrt{2(P_\phi+P_\psi)}}{\overline{H}+\overline{k_1}P_\phi+\overline{k_2}P_\psi},$$

one realizes immediately that when one of the actions increases greatly, $v_\perp \to 0$.

V. CONCLUSION

We have presented the basic physics underlying the scheme for generating currents in fusion plasmas and emphasizing its qualitative aspects. A quantitative evaluation of a practical current drive having its origin in the multiple AR acceleration mechanism described in this paper is presently under study and is planned to be reported in a future paper.

APPENDIX

In this appendix we show the complete integrability of the system of equations (19)–(22). As an introductory step we express in Eq. (20) the phase ψ in terms of the phase ϕ and the proper time using Eq. (23). Adding then Eqs. (21) and (22), we get

$$R'=-\overline{A_1}\cos\phi-\overline{A_2}\cos(\phi+c_0 s+\xi_0),$$

where $R=\sqrt{2(P_\phi+P_\psi)}$. Equation (20) will then read

$$\phi'=1-\overline{\omega_1}\overline{H^*}+\frac{\overline{A_1}\sin\phi+\overline{A_2}\sin(\phi+c_0 s+\xi_0)}{R}.$$

Now we perform the transformations $x=R\cos\phi$ and $y=R\sin\phi$. For these variables we get

$$x'=-y(1-\overline{\omega_1}\overline{H^*})-\overline{A_1}-\overline{A_2}\cos(c_0 s+\xi_0),$$

$$y'=x(1-\overline{\omega_1}\overline{H^*})+\overline{A_2}\sin(c_0 s+\xi_0),$$

from which we get

$$x''+(1-\overline{\omega_1}\overline{H^*})^2 x=\overline{A_2}[(2\overline{\omega_1}-\overline{\omega_2})\overline{H^*}-1]\sin(c_0 s+\xi_0),$$

which describes a driven harmonic linear oscillator system, which is of course completely integrable. In a similar manner, eliminating the phase ϕ in favor of the phase ψ, we get

$$X''+(1-\overline{\omega_2}\overline{H^*})^2 X=\overline{A_1}[1+(\overline{\omega_1}-2\overline{\omega_2})\overline{H^*}]\sin(c_0 s+\xi_0),$$

where now $X=R\cos\Psi$.

[1] A. A. Kolomenskii and A. N. Lebedev, Zh. Eksp. Teor. Fiz. **44**, 261 (1963) [Sov. Phys. JETP **17**, 179 (1963)].

[2] V. Ya. Davydovskii, Zh. Eksp. Teor. Fiz. **43**, 886 (1962) [Sov. Phys. JETP **16**, 629 (1963)].

[3] A. Yu. Kuyanov, A. A. Skovoroda, A. V. Timofeev, and A. V. Timofeev, and A. V. Zvonkov, *Proceedings of the Fourteenth International Conference on Plasma Physics and Controlled Nuclear Fusion Research* (IAEA, Vienna, 1992), Vol. 1, p. 733.

[4] A. I. Neishtadt and A. V. Timofeev, Zh. Eksp. Teor. Fiz. **93**, 1706 (1987) [Sov. Phys. JETP **66**, 973 (1987)].

[5] A. A. Balmashnov and K. S. Golovanivskii, Zh. Tekh. Fiz. **45**, 766 (1975) [Sov. Phys. Tech. Phys. **20**, 483 (1976)]; K. S. Golovanivskii, Phys. Scr. **22**, 126 (1980).

[6] L. Friedland, Phys. Plasmas **1**, 421 (1994).

[7] V. Ya. Davydovskii, Phys. Lett. A **147**, 226 (1990).

[8] Y. Gell and R. Nakach, Phys. Lett. A **207**, 342 (1995).

[9] C. Chen and G. Schmidt, Comments Plasma Phys. Controlled Fusion **12**, 83 (1988).

[10] B. V. Chirikov, Phys. Rep. **52**, 263 (1979).

[11] A. J. Lichtenberg and M. A. Lieberman, *Regular and Chaotic Dynamics*, 2nd ed. (Springer, New York, 1992), p. 288.

[12] Y. Gell and R. Nakach, Phys. Fluids B **4**, 368 (1992).